Int. J. Electrochem. Sci., 17 **(2022)** Article Number: 221010, doi: 10.20964/2022.10.05

International Journal of
ELECTROCHEMICAL
SCIENCE
www.electrochemsci.org

Short Communication

Highly Sensitive Enzyme-Free Electrochemical Sensor based on $Ni(OH)_2$/C Composite for the Detection of Blood Glucose

Ping Wang

School of Medicine and Nursing, Wuhan Railway Vocational College of Technology, Wuhan, Hubei 430205, China
E-mail: wangpingmedicine@163.com

Received: 30 May 2022 / *Accepted:* 17 July 2022 / *Published:* 10 September 2022

The current focus of electrochemical glucose sensors is on second-generation enzyme biosensors, i.e. portable glucose meters. This sensor uses an active biological enzyme's specific action to catalyze glucose oxidation to produce a current signal for detection purposes. The glucose oxidase enzyme used in this method is biologically active and, therefore, can significantly impact accuracy and produce errors in some environments. Also, when vitamin C, dopamine, and uric acid are outside the normal range for the body, they can interfere with the results. Therefore, it has become a hot research topic to try to study an enzyme-free sensor with less influence on external factors. In this work, a $Ni(OH)_2$/C electrode was prepared by the pressed sheet method, and its detection system was evaluated. The results demonstrate that this enzyme-free electrochemical sensor can detect glucose linearly between 1 mM and 11 mM. Meanwhile, this work investigated the practicality of this enzyme-free electrochemical sensor by comparing three commercially available portable glucose meters.

Keywords: Glucose analyzer; Enzyme-free, $Ni(OH)_2$; Portable sensor; Blood glucose

1. INTRODUCTION

With the improvement of people's living standards and the change in living environment, the number of people with diabetes is increasing yearly. Various acute and chronic complications caused by disorders of glucose metabolism pose a significant risk to human health. Blood glucose monitoring is an important part of diabetes management [1,2]. Blood glucose monitoring provides a better understanding of the patient's blood glucose changes and assesses the extent of the patient's glucose metabolism disorders [3]. This can be used to develop a rational glucose-lowering regimen, thus reducing the incidence of acute and chronic complications and morbidity and mortality in diabetic patients. Blood glucose testing is available in the laboratory with large automatic biochemical analyzers and portable glucose meter measurement methods [4–6]. The automated biochemistry analyzer determines venous

plasma or serum glucose results with accurate and reliable results with a high degree of precision and accuracy. However, because of its long testing time, complicated operation and cumbersome process, the automatic biochemical analyzer is not suitable for long-term glucose monitoring of patients [7,8]. A portable blood glucose meter has been widely used in the clinic and patients' families because of the advantages of convenience, speed, simple operation, and ease to grasp [9,10].

Portable glucose meters at this stage are enzyme-containing glucose electrochemical biosensors. However, as a type of electrochemical biosensor, the stability of the enzyme glucose sensor is influenced by the intrinsic enzyme is a drawback that is difficult to overcome as far as [11,12]. The activity of enzymes is also affected by temperature, pH of the solution, and toxic chemicals. Once the enzyme is affected by these, its biological activity decreases rapidly, eventually leading to a decrease in stability [13–15]. Therefore, developing enzyme-free electrochemical sensors is a challenge for portable glucose meters. It is also known that the relatively poor performance of enzyme-free sensors against interferences such as urea, uric acid, and ascorbic acid interferes with the analysis of biological samples and gives a false positive/negative result is also an important factor that hinders their development [16]. Enhancing the selectivity of electrodes has always been a significant challenge. To solve this problem, various materials have been fabricated as electrode surfaces or as electrode materials [17–19]. Some metal oxides and precious metals, such as gold, nickel hydroxide, porous copper oxide nanoparticles, manganese dioxide carbon nanotube composites, cobalt oxide, nickel oxide, and multi-walled carbon nanotubes, are commonly used in current-based glucose sensors [20].

According to current literature reports, Ni metal has the advantages of high stability and good reversibility, but the sensitivity is relatively low [21–24]. Since the kinetic reaction process of glucose and other interfering substances on the electrode surface is different, glucose is mainly controlled by the electrochemical reaction process, so this work chooses Ni metal with catalytic performance and good redox activity as the active material, together with carbon powder with excellent conductivity and more stable as the dispersion carrier [25–27]. This work increased the contact between the active substance on the electrode surface and the electrolyte by adding electron transfer channels on the electrode surface, thus increasing the sensitivity of glucose detection and reducing the error rate caused by the current response of interfering substances. Meanwhile, this work compared the prepared enzyme-free electrochemical sensor with a commercially available glucose meter.

2. EXPERIMENTAL

2.1. Reagents and instruments

$Ni(OH)_2$, KOH, acetylene black, glucose, and ammonium nitrate were purchased from Shandong West Asia Reagent, Tianjin Jinke Fine Chemical Research Institute, Cabot Ltd, Tianjin Guangfu Fine Chemical Research Institute, and Tianjin Huadong Reagent Factory, respectively. Polytetrafluoroethylene emulsion was purchased from Shanghai Hesen Electric Co., Ltd. with 60% mass fraction. Nickel foam is from Changsha Liyuan New Material Co., Ltd. with a purity of 99.5 wt%.

2.2. Preparation of electrode

(1) Pressing of electrodes: A certain amount of $Ni(OH)_2$ and 0.2 g of NH_4NO_3 were dispersed into 2 mL of a mixture of ethanol and water, then 0.2 g of polytetrafluoroethylene emulsion was added dropwise to this system. This mixture was then ultrasonically mixed well and added dropwise to 0.4 g of acetylene black. The already infiltrated acetylene black becomes a monolithic block by stirring, and this solid is rolled into a carbon sheet with a thickness of about 100-120 μm.

(2) Firing of electrodes: Starting from room temperature with a heating rate of 2°C/min to 120°C, the constant temperature was maintained for 2 h and naturally cooled down to room temperature to obtain $Ni(OH)_2$/C composites.

(3) Electrode pressing: The $Ni(OH)_2$/C composite sheet is cut into two carbon sheets of the same area and then placed on both sides of nickel foam with nickel foam in a sandwich structure and pressed together at 10 MPa.

The masses of $Ni(OH)_2$ added were 0.1, 0.15 and 0.2 g, and the mass ratios to carbon were 2:8, 3:8 and 4:8, respectively, named $Ni(OH)_2$/C-1, $Ni(OH)_2$/C-2 and $Ni(OH)_2$/C-3.

2.3. Detection of glucose

The glucose sensors were performed in 1, 3 and 6 M KOH solutions at a constant potential of 0.48 V. After the current is stabilized, a specific concentration of glucose solution is added every 20 s. The potential of the glucose solution was kept constant at 0.37, 0.39, 0.42, 0.48, and 0.55 V in 1 M KOH solution. The standard addition method has been applied to test the proposed electrochemical sensor and four commercially available glucose meters.

2.4. Information on commercially available electrochemical glucose meters

Three portable glucose meters were used for feasibility testing.

(1) Meter 1: The analytical principle used in this instrument is the glucose dehydrogenase electrochemical method. Detection range is 0.6-33.3 mM; sample blood volume is 0.6 uL; detection time is 5 s.

(2) Meter 2: The instrument adopts the analytical principle of the glucose dehydrogenase electrochemical method. Detection range is 1.1-27.8 mM; sample blood volume is 0.6 uL; detection time is 5 s.

(3) Meter 3: The instrument adopts the analytical principle of the glucose oxidase electrochemical method. The detection range is 1.1-33.3 mM; sample blood volume is 0.5 uL; detection time is 5 s.

3. RESULTS AND DISCUSSION

For electrodes made by mechanical pressing, the conductivity of the electrode surface and the adequacy of the contact between the active substance and the electrolyte determine the detection

performance of the electrode [28,29]. Therefore, it is particularly important to observe the electrode morphology, the pore distribution, and the loading of $Ni(OH)_2$. The SEM images of the electrodes are shown in Figure 1. It can be observed that the presence or absence of $Ni(OH)_2$ has a specific effect on the morphology of the electrode surface [30–32]. The surface of the electrode in the presence of $Ni(OH)_2$ is significantly finer than that of the electrode without $Ni(OH)_2$, and the surface of the electrode is closely and uniformly distributed with pore channels of about 150 nm in diameter connected by carbon particles. The pore structure is more conducive to the contact between $Ni(OH)_2$ on the carbon surface and the electrolyte, thus providing the electron transfer channel required for the rapid reaction of $Ni(OH)_2$. This allows the active material per unit area to oxidize more glucose per unit time and generate the corresponding electrochemical signal. The use of $Ni(OH)_2$/C composites as electrodes for detecting glucose has been reported [33]. Previous reports have also demonstrated that this material is a very promising electrode material that can be used to assemble of electrochemical sensors. In this work, the proposed sensor is not only characterized by morphological properties. The proposed sensor was also compared with a wide available glucose meter to verify its feasibility.

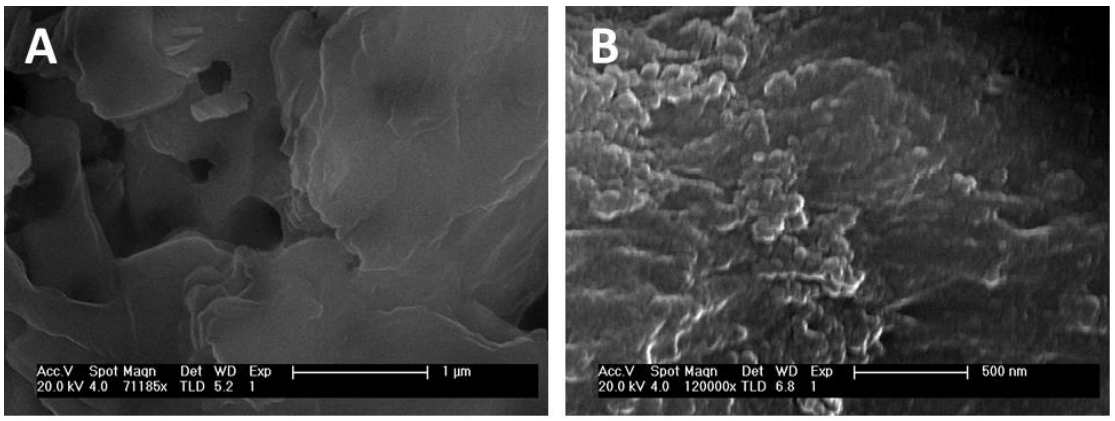

Figure 1. SEM image of (A) carbon electrode and (B) $Ni(OH)_2$/C.

This work kept the additions of acetylene black, ammonium nitrate, and PTFE emulsion consistent and varied the amount of $Ni(OH)_2$. The $Ni(OH)_2$/C-1, $Ni(OH)_2$/C-2, and $Ni(OH)_2$/C-3 electrodes, which were made with the mass ratio of $Ni(OH)_2$ to carbon powder of 2:8 3:8 4:8, were pre-activated by cyclic voltammetry (CV) in 1M KOH solution. The CV scan is used for activation of electrode, so that the material on the electrode surface reaches a steady-state (no analyte was added to the electrolyte). This is a standard electrode stability pretreatment for electrochemical sensors after preparation. Then, the sensors' sensing performance was tested by adding different glucose concentrations. The test results are shown in Figure 2. From the beginning of current stabilization, 100 µL of 500 mM glucose solution was added to the 50 mL electrolyte system every 20 s. The potential in this experiment has been optimized. The specific optimization details are shown in Figure 4. As shown figure, each addition of glucose causes a significant step in the current signal, and the current value will reach dynamic equilibrium within 5 s. Typically, as the active substance $Ni(OH)_2$ increases, its redox

reaction generates a higher background current [34]. However, the conclusion from the experimental results of constant potential oxidation of glucose at these three electrodes is that the current background decreases with the active substance's increase [35,36]. This may be due to keeping the same amount of emulsion, ammonium nitrate and toner added during the electrode fabrication process; the only thing that changes is the amount of active substance [37]. When the mass of $Ni(OH)_2$ is particularly small, the pore size of the electrode surface is relatively large instead, which is more conducive to the conduction of electrons. Moreover, the electrode's resistance is low because of $Ni(OH)_2$'s poor conductivity. Thus, when no glucose is added, relatively large currents can be generated at constant potential conditions [38]. When the background current is small, the net response current value generated when glucose is added will be more pronounced, and the electrode will be more sensitive to glucose detection. Therefore, combining the current background values with the net response current values generated when glucose was added, a $Ni(OH)_2$/C-3 electrode with a mass of 0.2 g of active substance was chosen for the following study.

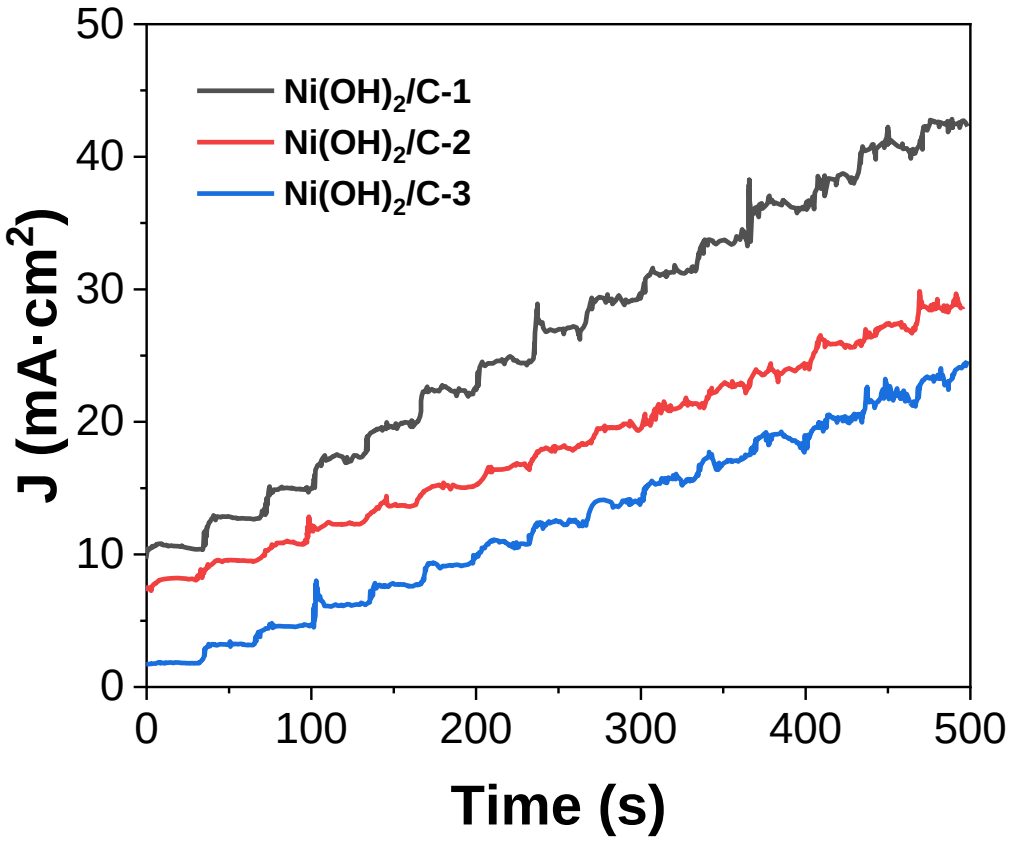

Figure 2. Chronoamperometry of $Ni(OH)_2$/C-1, $Ni(OH)_2$/C-2 ,$Ni(OH)_2$/C-3 in 1 M KOH at 0.48 V with addition of glucose (100 μL of 500 mM glucose solution each time).

Because an alkaline medium is a necessary medium for the oxidation of $Ni(OH)_2$ to NiOOH and thus glucose, this work investigated the effect of different concentrations of KOH (1M, 3M, and 6M) on the oxidation of glucose at the $Ni(OH)_2$/C electrode [39]. This work performed the chronoamperometry

test at a constant potential of 0.48 V. 100 μL of 500 mM glucose solution was added dropwise to the 50 mL system every 20 s starting from the time of current stabilization for a total of 15 drops. The experimental results are shown in Figure 3.

When the OH^- concentration in the system increases, the background current of the electrode increases. This may be due to the acceleration of the $Ni(OH)_2+OH^-\rightarrow NiOOH+H_2O+e$ reaction. As a result, its blank redox reaction is gradually more pronounced, and the generated current signal is gradually enhanced. However, the electrode is not only related to the OH^- concentration in the electrolyte when detecting glucose but also to the mass transfer rate of glucose to the electrode surface [40]. When the KOH concentration is too high, the resistance of glucose diffusion to the electrode surface is enhanced. This causes a decrease in the amount of glucose reaching the electrode surface per unit time, and therefore a decrease in sensitivity [41]. However, it is worth noting that the relative standard deviation of the corresponding linear fit curve is closer to 1 when the OH^- concentration in the electrolyte is higher for the same number of glucose additions.

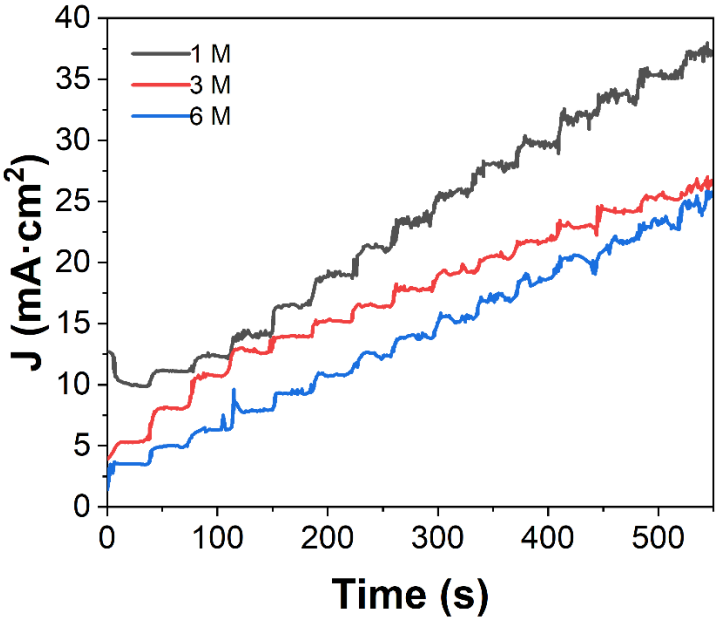

Figure 3. Chronoamperometry of $Ni(OH)_2$/C-3 electrode in 1M, 3 M and 6 M KOH electrolyte at 0.48 V with addition of glucose (100 μL of 500 mM glucose solution each time).

When an oxidation peak potential is applied to the working electrode, the divalent nickel ions in the electrode will be oxidized to trivalent nickel ions at its oxidation peak potential, and a background current will be generated at this time [42,43]. Because Ni is a powerful oxidizer, when glucose is added to the system, part of Ni oxidizes the glucose to gluconolactone. It is reduced to Ni again, at which point this reduced Ni continues to be oxidized to trivalent at the oxidation potential, resulting in a response current. Therefore, the increase in response current is proportional to the amount of glucose added, and the amount of glucose detected by the electrode can be obtained by calculating the change in response current [44]. Based on the results of glucose sensitivity assays performed in different concentrations of alkali environment, it is known that the sensitivity decreases with the increase of alkali concentration. It

may be because the viscosity of the electrolyte increases when the KOH concentration is higher. Since this electrode reaction is mainly controlled by diffusion, the viscosity of the electrolyte has a more significant effect on the mass transfer when the stirring rate is certain. The linear correlation coefficient increases with increasing electrolyte concentration because of the consumption of OH in the electrode process [45]. Therefore, 1 M KOH was chosen as the electrolyte considering the effect of increasing OH concentration on the reaction and the hindering effect on mass transfer.

This work further investigated the effect of test potentials on glucose detection. This work selected 0.55 V, 0.48 V, 0.48 V, 0.37 V and 0.39 V for testing the electrode's ability to oxidize glucose. The results of the chronoamperometry are shown below in Figure 4. According to the above experimental results, the linear correlation of the electrodes is poor at low potential (0.37 V, 0.39 V) conditions. This is because the content of nickel ions plays a decisive role in the linear detection range. When the concentration of OH^- is fixed, the interconversion rate between $Ni(OH)_2$ and NiOOH is slower at lower potentials, making the whole reaction process when glucose is detected at low potentials influenced by both mass transfer diffusion and electrochemical reaction rate [46]. On the contrary, at higher potentials, $Ni(OH)_2$ has a higher linear correlation due to the faster rate of oxidation to NiOOH. However, when the potential is too high (above 0.48 V), the precipitation competition reaction starts to be significantly larger than the oxidation reaction of $Ni(OH)_2$, thus causing a sharp increase in the background current and a smaller value of the oxidation response to glucose [47].

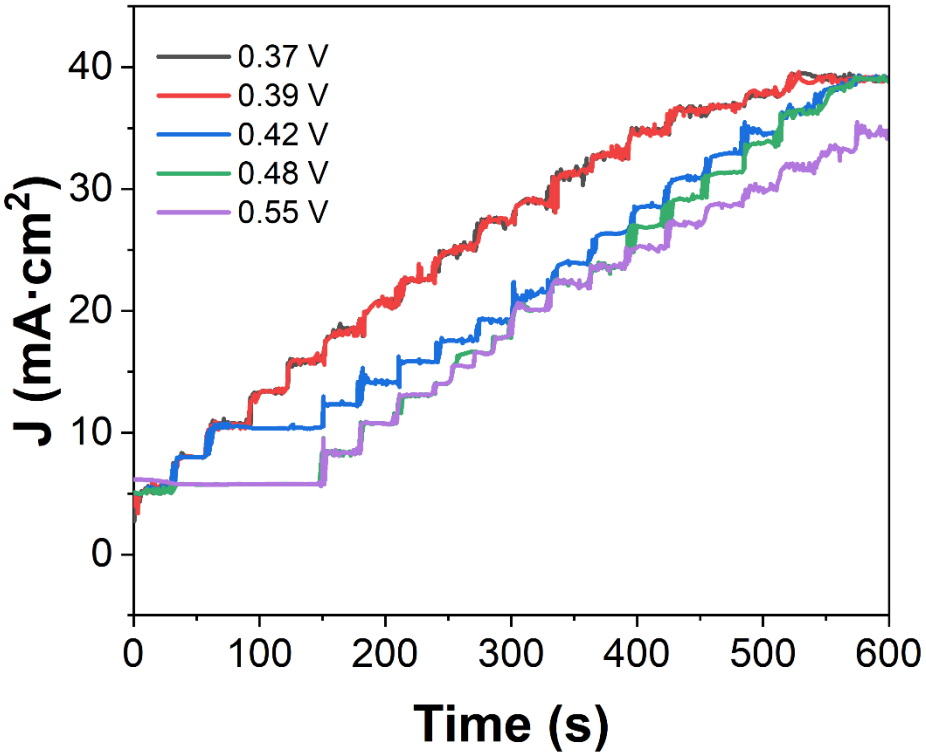

Figure 4. Chronoamperometry of $Ni(OH)_2$/C-3 electrode in 1M KOH electrolyte using 0.55 V, 0.48 V, 0.42 V, 0.37 V and 0.39 V as working potential with addition of glucose (100 μL of 500 mM glucose solution each time)..

Parallelism of electrodes is a prerequisite for the reliability of electrode test data and an important performance indicator for whether the electrodes can be widely used. This work randomly selected three $Ni(OH)_2$/C-3 electrodes made from the same batch and examined the differences in glucose detection data between the three different Schein electrodes at a constant potential of 0.48 V in 1 M KOH solution. Figure 5A shows the tested I-t curve, and Figure 5B shows the linear fit curve (current density-concentration curve).

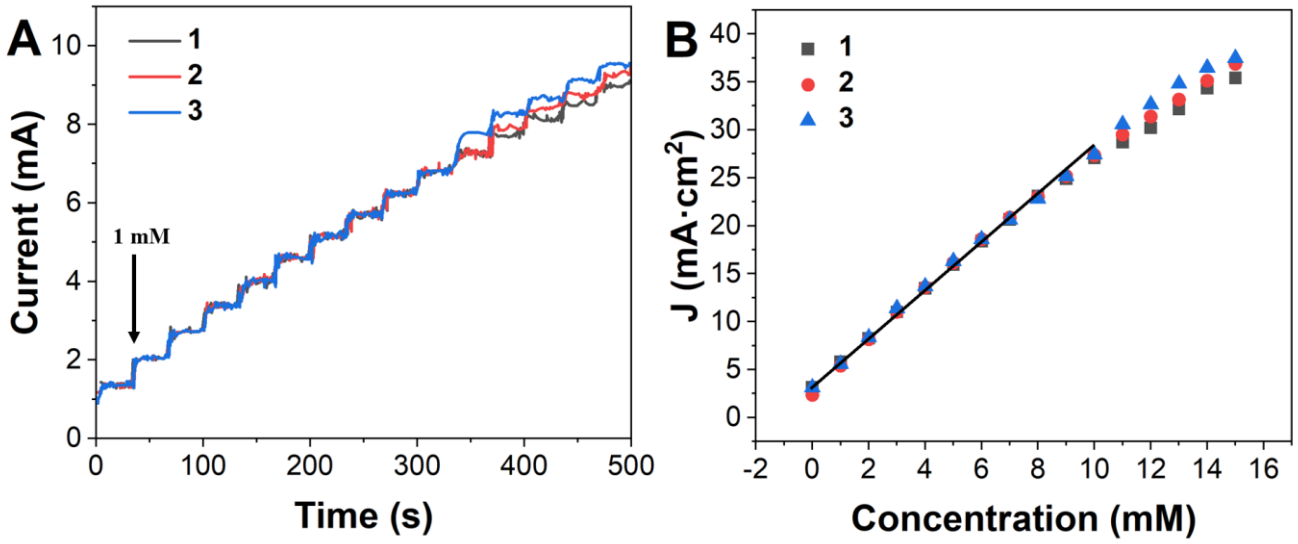

Figure 5. (A) Chronoamperometry of three individual $Ni(OH)_2$/C-3 electrodes with the addition of glucose in 1M KOH electrolyte at 0.48 V (1 mM each addition). (B) The relationship between the concentration of glucose against the current.

Table 1. Comparison of $Ni(OH)_2$/C-3 with previously reported glucose sensors.

Electrode	Linear range	LOD	Reference
NiO nanofibers	0.002-0.60 mM	0.77 mM	[48]
NiO/SCCNTs	0.002 to 2.2 mM	0.1 mM	[49]
NiO nanosheets	0.0005 to 2.31 mM	0.145 μM	[50]
$NiCo_2O_4$ nanorods	0.001 to 0.88 mM	0.063 μM	[51]
$NiCo_2O_4$ nanobelt/Ni foam	0.0009 to 0.067 mM	0.9 μM	[52]
SiO_2/GO/GCE	0 to 900 μM	0.03 μM	[53]
$Ni(OH)_2$/C-3	1 to 11 mM	0.6 mM	This work

The information in the figure shows that there is no great difference in the response of the electrodes to glucose when the number of drops of glucose added to the system is small (1 to 11 times). The current density-glucose concentration of the three electrodes can be linearly related when the

glucose concentration in the system ranges from 1 mM to 11 mM. The three electrodes started to show significant differences when glucose was continued to be added dropwise until the concentration of glucose in the system exceeded 11 mM. The detection limit can be calculated as 0.6 mM. The overall analytical performance of the $Ni(OH)_2$/C-3 was compared with the previous literature (see Table 1). It can be seen that the proposed sensor is more competitive in the detection of high concentrations of blood glucose.

This work further analyzed the blood glucose bias of the three medium enzyme-containing blood glucose meters and our proposed enzyme-free blood glucose testing technique. The standard addition method has been applied to test the feasibility of the proposed electrochemical sensor with commercial glucose meters. The results are shown in Table 2. It can be seen from the above two tables that the proposed $Ni(OH)_2$/C-3 is a very competitive electrochemical sensor, which is comparable to the commercial glucose meter.

Table 2. Sensing performance of $Ni(OH)_2$/C-3 with four blood glucose meter.

Sensor	Found (mM)	Added (mM)	Found (mM)	Recovery (%)
$Ni(OH)_2$/C-3	2.71	1.00	3.73	100.54
Meter 1	2.68	1.00	3.72	101.09
Meter 2	2.72	1.00	3.79	101.88
Meter 3	2.68	1.00	3.65	99.18

4. CONCLUSION

This work prepared $Ni(OH)_2$/C composite electrodes with multi-pore channels by choosing Ni metal with catalytic properties and good redox activity as the active material by the pressed sheet method. The electrode can detect blood glucose as an enzyme-free electrochemical sensor. The electrode has good linearity and sensitivity at a detection potential of 0.48 V in 1 M KOH solution. The proposed enzyme-free electrochemical sensor was used with three portable glucose meters to measure fixed fasting and 2-hour post-glucose load glucose. The results showed a good correlation between the enzyme-free electrochemical sensor and biochemical analyzer results, indicating the potential of this enzyme-free sensor for practical applications.

References

1. H. Yoon, J. Nah, H. Kim, S. Ko, M. Sharifuzzaman, S.C. Barman, X. Xuan, J. Kim, J.Y. Park, *Sens. Actuators B Chem.*, 311 (2020) 127866.
2. J. Dai, H. Zhang, C. Huang, Z. Chen, A. Han, *Anal. Chem.*, 92 (2020) 16122–16129.
3. E.G. Wilmot, M. Evans, K. Barnard-Kelly, M. Burns, I. Cranston, R.A. Elliott, G. Gkountouras, N. Kanumilli, A. Krishan, C. Kotonya, *BMJ Open*, 11 (2021) e050713.
4. P. Mandpe, B. Prabhakar, H. Gupta, P. Shende, *Sens. Rev.* (2020).
5. J. Liu, X. Shen, D. Baimanov, L. Wang, Y. Xiao, H. Liu, Y. Li, X. Gao, Y. Zhao, C. Chen, *ACS Appl.*

Mater. Interfaces, 11 (2018) 2647–2654.
6. H. Karimi-Maleh, Y. Orooji, F. Karimi, M. Alizadeh, M. Baghayeri, J. Rouhi, S. Tajik, H. Beitollahi, S. Agarwal, V.K. Gupta, *Biosens. Bioelectron.*, 184 (2021) 113252.
7. Y. Yao, J. Chen, Y. Guo, T. Lv, Z. Chen, N. Li, S. Cao, B. Chen, T. Chen, *Biosens. Bioelectron.*, 179 (2021) 113078.
8. L. Tang, S.J. Chang, C.-J. Chen, J.-T. Liu, *Sensors*, 20 (2020) 6925.
9. D. Tankasala, J.C. Linnes, *Transl. Res.*, 213 (2019) 1–22.
10. H. Karimi-Maleh, A. Khataee, F. Karimi, M. Baghayeri, L. Fu, J. Rouhi, C. Karaman, O. Karaman, R. Boukherroub, *Chemosphere*, 291 (2021) 132928.
11. M. Zhao, P.S. Leung, *Future Med. Chem.*, 12 (2020) 645–647.
12. Y. Chen, X. Jiang, J. Wang, Z. Wu, Y. Wu, Z. Ni, H. Yi, R. Lu, *Anal. Chem.*, 93 (2021) 14153–14160.
13. Q. Cao, B. Liang, T. Tu, J. Wei, L. Fang, X. Ye, *RSC Adv.*, 9 (2019) 5674–5681.
14. J.R. Sempionatto, J.-M. Moon, J. Wang, *ACS Sens.*, 6 (2021) 1875–1883.
15. H. Karimi-Maleh, F. Karimi, L. Fu, A.L. Sanati, M. Alizadeh, C. Karaman, Y. Orooji, *J. Hazard. Mater.*, 423 (2022) 127058.
16. V.P. Rachim, W.-Y. Chung, *Sens. Actuators B Chem.*, 286 (2019) 173–180.
17. P. Mohammadnejad, S.S. Asl, S. Aminzadeh, K. Haghbeen, *Spectrochim. Acta. A. Mol. Biomol. Spectrosc.*, 229 (2020) 117897.
18. D. Li, R. Tan, X. Mi, C. Fang, Y. Tu, *Microchem. J.*, 167 (2021) 106271.
19. H. Karimi-Maleh, M. Alizadeh, Y. Orooji, F. Karimi, M. Baghayeri, J. Rouhi, S. Tajik, H. Beitollahi, S. Agarwal, V.K. Gupta, S. Rajendran, S. Rostamnia, L. Fu, F. Saberi-Movahed, S. Malekmohammadi, *Ind. Eng. Chem. Res.*, 60 (2021) 816–823.
20. Z. Peng, X. Xie, Q. Tan, H. Kang, J. Cui, X. Zhang, W. Li, G. Feng, *J. Innov. Opt. Health Sci.*, 15 (2022) 2230003.
21. B.J. Van Enter, E. Von Hauff, *Chem. Commun.*, 54 (2018) 5032–5045.
22. D. Rodin, M. Kirby, N. Sedogin, Y. Shapiro, A. Pinhasov, A. Kreinin, *Clin. Biochem.*, 65 (2019) 15–20.
23. F.F. Franco, R.A. Hogg, L. Manjakkal, *Biosensors*, 12 (2022) 174.
24. H. Karimi-Maleh, H. Beitollahi, P.S. Kumar, S. Tajik, P.M. Jahani, F. Karimi, C. Karaman, Y. Vasseghian, M. Baghayeri, J. Rouhi, *Food Chem. Toxicol.* (2022) 112961.
25. X. Cui, J. Li, Y. Li, M. Liu, J. Qiao, D. Wang, H. Cao, W. He, Y. Feng, Z. Yang, *Spectrochim. Acta. A. Mol. Biomol. Spectrosc.*, 266 (2022) 120432.
26. K. Jang, K.R. Park, K.M. Kim, S. Hyun, C. Ahn, J.C. Kim, S. Lim, H. Han, S. Mhin, *Appl. Surf. Sci.*, 545 (2021) 148927.
27. F. Wang, X. Niu, W. Wang, W. Jing, Y. Huang, J. Zhang, *J. Taiwan Inst. Chem. Eng.*, 93 (2018) 87–93.
28. M. Wang, D. He, M. Huang, X. Wang, P. Jiang, *J. Alloys Compd.*, 786 (2019) 530–536.
29. S.H. Lee, M.S. Kim, O.-K. Kim, H.-H. Baik, J.-H. Kim, *J. Nanosci. Nanotechnol.*, 19 (2019) 6187–6191.
30. J. Ye, D. Deng, Y. Wang, L. Luo, K. Qian, S. Cao, X. Feng, *Sens. Actuators B Chem.*, 305 (2020) 127473.
31. G. Han, S. Chen, X. Wang, J. Wang, H. Wang, Z. Zhao, *Infrared Phys. Technol.*, 113 (2021) 103620.
32. H. Karimi-Maleh, A. Ayati, S. Ghanbari, Y. Orooji, B. Tanhaei, F. Karimi, M. Alizadeh, J. Rouhi, L. Fu, M. Sillanpää, *J. Mol. Liq.*, 329 (2021) 115062.
33. L. Wang, Y. Tang, L. Wang, H. Zhu, X. Meng, Y. Chen, Y. Sun, X.J. Yang, P. Wan, *J. Solid State Electrochem.*, 19 (2015) 851–860.
34. C. Sabu, T. Henna, V. Raphey, K. Nivitha, K. Pramod, *Biosens. Bioelectron.*, 141 (2019) 111201.
35. J. Shan, J. Li, X. Chu, M. Xu, F. Jin, X. Wang, L. Ma, X. Fang, Z. Wei, X. Wang, *RSC Adv.*, 8 (2018) 7942–7948.
36. H. Karimi-Maleh, A. Ayati, R. Davoodi, B. Tanhaei, F. Karimi, S. Malekmohammadi, Y. Orooji, L.

Fu, M. Sillanpää, *J. Clean. Prod.*, 291 (2021) 125880.
37. P. Chakraborty, S. Dhar, K. Debnath, T. Majumder, S.P. Mondal, *Sens. Actuators B Chem.*, 283 (2019) 776–785.
38. X. Wang, F. Li, Z. Cai, K. Liu, J. Li, B. Zhang, J. He, *Anal. Bioanal. Chem.*, 410 (2018) 2647–2655.
39. A. Yu, Z. Zeng, Q. Luo, J. Gao, Q. Wang, *Appl. Surf. Sci.*, 462 (2018) 883–889.
40. A. Ebrahimi, J. Scott, K. Ghorbani, *Sens. Actuators Phys.*, 301 (2020) 111662.
41. N. Gao, H. You, *BioChip J.*, 15 (2021) 23–41.
42. P. Lv, H. Zhou, A. Mensah, Q. Feng, D. Wang, X. Hu, Y. Cai, L.A. Lucia, D. Li, Q. Wei, *Chem. Eng. J.*, 351 (2018) 177–188.
43. S. Zhao, D. Guo, Q. Zhu, W. Dou, W. Guan, *Biosensors*, 11 (2020) 13.
44. A. Uzunoglu, D.A. Kose, E. Gokmese, F. Gokmese, *J. Clust. Sci.*, 31 (2020) 231–239.
45. S.K. Yee, S.C.J. Lim, P.S. Pong, S.H. Dahlan, *Prog. Electromagn. Res. C*, 99 (2020) 35–48.
46. Y. Wang, T. Wang, *Appl. Sci.*, 10 (2020) 3227.
47. J.S. Park, J.S. Choi, *Sens. Actuators B Chem.*, 359 (2022) 131585.
48. Y. Zhang, Y. Wang, J. Jia, J. Wang, *Sens. Actuators B Chem.*, 171 (2012) 580–587.
49. M.H. Raza, K. Movlaee, Y. Wu, S.M. El-Refaei, M. Karg, S.G. Leonardi, G. Neri, N. Pinna, *ChemElectroChem*, 6 (2019) 383–392.
50. M. Guo, L. Wei, Y. Qu, F. Zeng, C. Yuan, *Mater. Lett.*, 213 (2018) 174–177.
51. M. Saraf, K. Natarajan, S.M. Mobin, *New J. Chem.*, 41 (2017) 9299–9313.
52. X. Zhang, R. Wang, Y. Wei, X. Pei, Z. Zhou, J. Zhang, R. Zhang, D. Zhang, *Int. J. Electrochem. Sci.*, 16 (2021) 210465.
53. W. Sun, S. Yu, J. Liu, Y. Ke, J. Sun, *Int. J. Electrochem. Sci.*, 16 (2021) 210220.